JPET Fast Forward. Published on December 31, 2020 as DOI: 10.1124/jpet.120.000427
This article has not been copyedited and formatted. The final version may differ from this version.

1. TITLE PAGE

Novel Tocolytic Strategy: Modulating Cx43 Activity by S-Nitrosation

Scott D. Barnett, Hazik Asif, Mitchell Anderson, and Iain L. O. Buxton

Department of Pharmacology, Center for Molecular Medicine, University of Nevada,

Reno School of Medicine, Reno, NV 89557

2. RUNNING TITLE PAGE

Running Tittle: Cx43 Activity and Modulation in the Myometrium

Address for Correspondence:

Scott D. Barnett, Ph.D.
Department of Pharmacology
University of Nevada Reno, School of Medicine
1664 N. Virginia Street (MS 318)
Reno, NV 89557
Ph: 775-682-7425
Fax: 775-784-1620
sdbarnett@med.unr.edu

# of text pages = 26 (intro - discussion), 38 total

# of figures = 6 + 2 supplmental (8)

# of references = 47

# of words in Abstract = 217

# of words in Introduction = 513

# of words in Discussion = 1495

Non-Standard Abbreviations

18β-GA - 18β-glycyrrhetinic acid

Cx43 - connexin 43

CAP - contractile associated protein

GJC - gap junction channel

GSNO - s-nitrosoglutathione

JPET Fast Forward. Published on December 31, 2020 as DOI: 10.1124/jpet.120.000427
This article has not been copyedited and formatted. The final version may differ from this version.

HC - hemichannel

NO - nitric oxide

NP - non-pregnant

OT - oxytocin

PTB - preterm birth

PTL - preterm labor

PTNL - preterm non-labor

SNO - s-nitrosothiol

sPTL - spontaneous preterm labor

TL - term labor

TNL - term non-labor

Recommended Section Assignment for JPET

1) Drug Discovery and Translational Medicine

JPET Fast Forward. Published on December 31, 2020 as DOI: 10.1124/jpet.120.000427
This article has not been copyedited and formatted. The final version may differ from this version.

3. ABSTRACT

Currently available tocolytics are ineffective at significantly delaying preterm birth. This is due in part to our failure to better understand the mechanisms that drive spontaneous preterm labor (sPTL). Cyclic nucleotides are not the primary contributors to myometrial quiescence, but instead nitric oxide (NO)-mediated protein S-nitrosation (SNO) is integral to the relaxation of the tissue. Connexin-43 (Cx43), a myometrial 'contractile associated protein' (CAP) that functions as either a gap junction channel (GJC) or an hemichannel (HC), was the focus of this study. Protein analysis determined that Cx43 is downregulated in sPTL myometrium. Further, Cx43 is S-nitrosated by NO, which correlates to an increase of Cx43-pS368 (gap junction inhibition), as well as an increase in the hemichannel (HC) open-state probability (quiescence). Pharmacologic inhibition of Cx43 with 18β-Glycyrrhetinic acid (18β-GA) exhibits a negative inotropic effect on the myometrium in a dose-dependent manner, as does administration of nebivolol, a nitric oxide synthase (NOS) activator that increases total protein SNOs. When 18β-GA and nebivolol were co-administered at their IC_{50} values, the effect on contractile dynamics was additive, all but eliminating contractions. The development of new tocolytics demands a better understanding of the underlying mechanisms of sPTL. Here it has been shown that 18β-GA and nebivolol leverage dysregulated pathways in the myometrium, resulting in a novel approach for the treatment of sPTL.

JPET Fast Forward. Published on December 31, 2020 as DOI: 10.1124/jpet.120.000427
This article has not been copyedited and formatted. The final version may differ from this version.

4. Significance Statement

While there are many known causes of preterm labor (PTL), the mechanisms of 'spontaneous' preterm labor (sPTL) remain obfuscated, which is why treating this condition is so challenging. Here we have identified that Cx43, an important contractile-associated protein, is dysregulated in sPTL myometrium, and that the pharmacologic inhibition of Cx43, and its S-nitrosation, with 18β-GA and nebivolol, respectively, significantly blunts contraction in human myometrial tissue, presenting a novel approach to tocolysis that leverages maladjusted pathways in women who experience sPTL.

JPET Fast Forward. Published on December 31, 2020 as DOI: 10.1124/jpet.120.000427
This article has not been copyedited and formatted. The final version may differ from this version.

6. INTRODUCTION

Seventy-five years of tocolytic development(Vanbésien and Eichner, 1956) has produced little in terms of effective therapies to halt preterm labor (PTL) or delay preterm birth (PTB)(WHO, 2015). This is concerning not only for the more than 15-million infants born prematurely each year, many of whom will experience lifelong health complications, such as chronic lung and cardiovascular disease, but also because PTL/PTB imparts in a substantial financial burden on the health care industry, costing greater than 40-billion annually (adjusted) in the United States alone(Behrman and Butler, 2007). It is clear that new strategies must be employed to mitigate this obstetric dilemma.

In contrast to most smooth muscle types, cyclic nucleotides (cGMP/cAMP) are not the dominant mediators of myometrial quiescence(Bradley *et al.*, 1998; Lai *et al.*, 2016; Barnett *et al.*, 2018). Interestingly, non-diseased myometrium will readily relax to nitric oxide (NO), whose canonical action in most smooth muscle types lies in cGMP/PKG activation, but whose primary actions differ in the myometrium through protein S-nitrosation. It is well established that NO-mediated protein S-nitrosation (SNO) imparts a wide range of effects on the cell, and that the disparate regulation of SNOs correlates to dozens of diseases(Foster *et al.*, 2003; Barnett and Buxton, 2017). Protein S-nitrosations are not only dysregulated in the myometrium of sPTL patients(Ulrich *et al.*, 2012), but the functional effect of these SNOs on contractile associated proteins (CAPs) underlies uterine quiescence(Barnett *et al.*, 2018).

JPET Fast Forward. Published on December 31, 2020 as DOI: 10.1124/jpet.120.000427
This article has not been copyedited and formatted. The final version may differ from this version.

Connexin-43 (Cx43) is a member of large family of connexins and pannexins which actively mediate cell-cell communication(Söhl and Willecke, 2004), including the myometrium(Pierce *et al.*, 2002). Cx43 functions as either a hemi-channel (HC), where it promotes quiescence through the permeation of prostaglandin-E_2(Burra and Jiang, 2009) and other low molecular weight molecules(Hansen *et al.*, 2014) from the cell, or as two such HCs in apposing membranes combining to form a gap junction channel (GJC), where it couples cells electrically to facilitate the propagation of contractile signals. The GJC/HC transition is largely driven by C-terminal phosphorylations(Leithe *et al.*, 2018), and in some cell types HC and GJC permeation is altered by its S-nitrosation (SNO) state, particularly by nitrosation of cysteine 271 (C271)(Straub *et al.*, 2011). Given that conditions promoting the Cx43 HC state and GJC inhibition may serve to facilitate myometrial quiescence, here we have elected to explore the functional consequences of S-nitroso regulation of Cx43 in human myometrium.

The conspicuous dearth of tocolytic strategies is due in part to our collective failure to better understand the mechanisms that underlie the biochemical regulation of uterine smooth muscle relaxation. Both the cGMP-independence of myometrial relaxation to NO(Bradley *et al.*, 1998), and the dysfunction of preterm laboring myometrium to NO-mediated relaxation(Barnett *et al.*, 2018), are known. What drives spontaneous preterm labor (sPTL) is not. The importance of NO-mediated protein S-nitrosation in the myometrium during pregnancy, coupled with the critical nature of Cx43 as a myometrial contraction-associated protein (CAP), makes Cx43 an attractive target of study. Here we investigate the regulation of Cx43 during

JPET Fast Forward. Published on December 31, 2020 as DOI: 10.1124/jpet.120.000427
This article has not been copyedited and formatted. The final version may differ from this version.

pregnancy/parturition, the effect of NO on Cx43 function, as well as the tocolytic potential for therapeutics that mediate SNOs and Cx43 activity.

7. MATERIAL AND METHODS

Tissue collection: Human tissue collection has been carried out in accordance with the Declaration of Helsinki and approved by the Institutional Review Board at the University of Nevada Biomedical Review Committee for the protection of human subjects. Human uterine biopsies were obtained with written informed-consent from mothers with singleton pregnancies undergoing Cesarean section without known infection or rupture of membranes (PROM/PPROM), as previously described(Barnett *et al.*, 2018). All experiments were performed in accordance with the NIH guidance on the use of human tissues in research. Exclusion criteria include age < 18 years, any history of drug abuse, co-morbid diagnoses such as HIV infection or AIDS, hepatitis C infection, uncontrolled diabetes, renal disease, preeclampsia, IUGR, placenta previa and any use of steroids other than betamethasone including topical use during pregnancy. SARS-CoV-2 positive patients were also excluded from this study. Tissues were transported to the laboratory immediately in cold Krebs buffer containing, in mM: NaCl (118), KCl (4.75), CaCl2 (2.5), KH2PO4 (1.2), NaHCO3 (25), MgCl2 (1.2), dextrose (20), and adjusted to pH 7.4. Tissues were dissected under magnification to isolate smooth muscle, employed in contractile experiments or snap frozen in liquid nitrogen (LN_2), and stored at -150 °C. Pregnant laboring patients ranged from 39 to 41 wk. gestation, with the mean at 39 wk. Preterm

JPET Fast Forward. Published on December 31, 2020 as DOI: 10.1124/jpet.120.000427
This article has not been copyedited and formatted. The final version may differ from this version.

laboring patients without evidence of infection, PROM or preeclampsia ranged from 29.2 to 36 wk. of gestation, with the mean being 33.6 wk.

Animal studies were approved by the University Institutional Animal Care and Use Committee. All experiments were conducted in accordance with the NIH guidelines for the use of vertebrate animals in research. Inbred Dunkin-Hartley Guinea pigs (Elm Hill, Chelmsford, MA) were purchased as either virgin juveniles (300–350 g) and bred on site, or as timed-pregnancies (30–35d). Non-pregnant guinea pigs were estrogen primed (3 mg/kg β-estradiol) 48-hours prior to tissue collection to ensure alignment of estrous cycles. Virgin female guinea pigs, and timed-pregnant animals, were sacrificed under isoflurane anesthesia.

Western Blot: Protein was isolated in MAPK buffer containing, in mM: Tris-HCL pH 6.8 (60), glycerol (1%), SDS (2%), leupeptin (0.001), EGTA (1) EDTA (1), AEBSF (1), Na_3VO_4 (1), and protease/phosphatase inhibitors (PPC110: Sigma Aldrich, St. Louis, MO). Samples were crushed using LN_2 w/ mortar and pestle, followed by 5 minutes in a tissue homogenizer. Sample concentrations were determined using EZQ (R33200: Thermo Fischer, Waltham, MA). Note - ‘n’s were not equal for all conditions due to an scarcity of samples, particularly sPTL.

For Cx43 total protein, 40 µg of protein lysate was run at 200 V for 45 min on a 4-20% PAGE gel and transferred to nitrocellulose, blocked in Licor® blocking buffer. The Western blot was labeled with mouse anti-Cx43 polyclonal 1° (1:1000, CX-1B1: Thermo Fischer, Waltham, MA), followed by either Alexa Fluor 680-donkey anti-mouse 2° (1:25k, ab175774: Abcam, Cambridge, MA) or IRDye 800-donkey anti-mouse 2° (1:25k, ab216774: Abcam, Cambridge, MA). Cx43 expression was

JPET Fast Forward. Published on December 31, 2020 as DOI: 10.1124/jpet.120.000427
This article has not been copyedited and formatted. The final version may differ from this version.

normalized to rabbit anti-GAPDH (1:1000, 2118S: Cell Signaling Technology, Danvers, MA) followed by either Alexa Fluor 680-goat anti-rabbit 2° (1:25k, ab216773: Abcam, Cambridge, MA) or IRDye 800-donkey anti-Rabbit (1:25k, 926-32213: Licor Biotechnology, Lincoln, NE). For pS368:S368 blots we used rabbit anti-pS368-Cx43 1° (1:1000, ab30559: Abcam, Cambridge, MA) and IRDye 800-goat anti-rabbit 2° (1:25k, ab216773: Cambridge, MA), followed by mouse anti-Cx43 polyclonal 1° (1:1000, CX-1B1: Thermo Fischer, Waltham, MA) and Alexa Fluor 680-donkey anti-mouse 2° (1:25k, ab175774: Cambridge, MA). S-nitrosated proteins gels were run as described above with 30 µl of eluted total-SNO proteins (see biotin switch method) with either a reversible 680 nm total proteins stain, Licor Revert™ (p/n 926-11010: Licor, Lincoln, NE), or with the Cx43 antibody described above.

Contractile studies: Strips of myometrium (~0.5 × 15 mm) were clip-mounted to a force transducer, and isometrically stretched to an initial tension of 1.2 × tissue length in an organ bath (DMT 820MS, Ann Arbor, MI) containing Krebs buffer(Barnett *et al.*, 2018). Tissues were maintained at 37 °C and gently bubbled with balanced oxygen (95% O2, 5% CO2). Tissues were then challenged with KCL (60 mM replacing NaCl) for 3 min, followed by wash-out, then allowed to equilibrate for 1 hr., during which time regular spontaneous contractions were seen. Only tissues that responded to KCL-challenge were employed in experiments. Under some conditions, tissues were further challenged with oxytocin (OT, 8 nM), followed by washout. Tissues served as their own controls based on tension prior to addition of drug. Data were analyzed with LabChart (version 8.1.12, Win10, ADInstruments., Colorado Springs, CO).

JPET Fast Forward. Published on December 31, 2020 as DOI: 10.1124/jpet.120.000427
This article has not been copyedited and formatted. The final version may differ from this version.

Biotin Switch and Streptavidin Pulldown: Myometrial tissue samples (n=4 patients) were hung in a tissue bath (see *contractile studies*) and exposed to either oxytocin (8 nM, 3 strips per patient) or oxytocin followed ~10 minutes later by GSNO (300 µM, 3 strips per patient) at the start of a contraction, then snap frozen with LN_2 at either peak contraction or maximal relaxation and stored in amber tubes (to protect S-nitrosation) at -150°C. Proteins were initially isolated in MAPK buffer with 2% SDS (see *western blot*). For the biotin switch(Jaffrey and Snyder, 2001), 1397 µg of total protein per sample was then suspended in HEN buffer containing, in mM: HEPES (25), EDTA (1), neocuproine (0.1), pH 7.7. An additional 2.5% SDS (final) and 30 mM N-ethylmaleimide (NEM) were added to block free thiols. Samples were incubated at 50°C in the dark for 20 minutes with frequent vortexing. (3) volumes of -30°C 100% acetone were added to each sample, and proteins were precipitated at -30°C overnight and collected by centrifugation at 3,000xg for ten minutes. After rinsing with 70% acetone protein pellets were dried using dry Nitrogen, then re-suspended in HENS (HEN + 1% SDS) with 10 mM ascorbate (to reduced SNO proteins) and 0.25 mg/ml biotin-HPDP (No. 16459: Cayman Chemical, Ann Arbor, MI) and rotated at room temperature for 1 hour. Proteins were precipitated and rinsed as before, and resuspended in a mixture of HENS (25%, 87 µl), neutralization buffer (50%, 174 µl) containing, in mM: HEPES (25), NaCl (100), EDTA (1), 0.5% Triton X-100, pH 7.5, and 75 µl of magnetic streptavidin beads (spherotech svmx-10-10, Lake Forest, IL). Samples were washed 5 times with (10) volumes of neutralization buffer in a magnetic stand, then recovered in 35 µl elution buffer containing a 1:10 dilution of HENS/H_2O with 1% v/v β-mercaptoethanol. Note - two

JPET Fast Forward. Published on December 31, 2020 as DOI: 10.1124/jpet.120.000427
This article has not been copyedited and formatted. The final version may differ from this version.

proteins pellets from GSNO treated samples were lost during a rinse phase and excluded from the data set.

Cell Culture: Human Embryonic Kidney (HEK293, p10-p25 - ATCC, Manassas, VA) and telemorized pregnant human uterine smooth muscle cells (phUSMC, p20-p30 - created in-house(Heyman *et al.*, 2013)) were grown in Dulbecco's modified Eagle's medium (DMEM) with 50 U/ml streptomycin, 50 µg/ml penicillin, and 10% FBS. phUSMC cells were further supplemented with estrogen (15 ng/ml) and progesterone (200 ng/ml). All cells were cultured in a balanced oxygen (95% O_2, 5% CO_2) 37°C incubator.

Ethidium Bromide Assay: HEK293 and phUSMC cells were seeded (~2500 cells/well) in 96-well plates (94.6000.024, Lumox Multiwell: Sarstedt, Newtown, NC) and grown to ~50-80% confluency. Experimental protocol was modified from(Contreras *et al.*, 2003). 24-48 hours after seeding the medium was exchanged for HEPES-buffered Krebs-Ringer (-) Ca^{2+} solution containing, in mM: NaCl (120), KCl (5), $MgCl_2$ (1), $NaHCO_3$ (25), HEPES (5.5), and D-glucose (1.1), pH 7.4, ± $CaCl_2$ (2.5, as dictated by experiment). 10 µM ethidium bromide (EtBr) was added to each well ± GSNO (300 µM) or TAT-Gap19 (100 µM, a membrane permeable Cx43 HC inhibitor) then returned to the cell culture incubator for 5 minutes. Following this, all wells were rinsed 3x with 37°C HEPES-buffered Krebs-Ringer (-) Ca^{2+}. This was denoted at t=0, and the plates were returned to the incubator. At each experimental time point (0,30,60, or 90 minutes), treated cells were exposed to paraformaldehyde to halt progression of EtBr intercalation, then rinsed 3x with buffer. Each well was then treated with DAPI (for cell counts), followed by 3x rinses. Plates were imaged

on an ImageExpress® Nano (Molecular Devices, San Jose, Ca) at 4x using MetaExpress® software (v.6.5.4.532) at a fixed exposure time of 1500 ms. Data collection and analysis was limited to a square in the middle of each well covering 32.63% with an average of 1024 cells to avoid incorporation of anomalous growth patterns common near the periphery of plates. Plate images in Figure 3 are magnified 6.8x (300x300px) and false colored (blue, DAPI: green, EtBr) to better visualize EtBr uptake, but were analyzed using the full scan with ImageJ (v. 2.0.0-rc-69/1.52p). Cell counts were determined by setting an appropriate threshold, followed by "Analyze Particles" (size=100-Infinity) on the DAPI channel. EtBr uptake was determined by "area fraction" of the EtBr channel using fixed threshold to avoid altering the analyzed signal from well to well. Area fractions were normalized to cell count, then each normalized area fraction was further normalized to the area fraction of the negative control [(-) EtBr] at each time point to account for noise in the background signal. t=0 was set to 'zero' and data is displayed as a fold-increase in fluorescent signal from t=0.

Statistical Analysis: For organ bath experiments (figures 2, 4, and 6) in which multiple tissue strips per patient were tested, each subsampling was pooled into a single 'n', and each data set consists of 3 to 5 patients ('n's, see results for specific values) except for when control tissue was non-viable for the full experimental duration, in which case the data was collected from a new sample. Each 'n' is signified as a tick on the graph's x-axis, and the overlayed bar graph signifies the nested mean with 95% confidence intervals (CI) error bars. Area Under the Curve (AUC) is defined as the period from the beginning to end of each contractile period.

The last three contractions of each dosing and control period were analyzed. Peak tension is defined as the maximum tension at the height of contraction and subtracted from the minimum tension for each given contraction. Each tissue strip was normalized to its own baseline prior to dosing, then to the average of all control strips (controls are vol. equivalents of drug solvent; EtOH for 18β-GA, DMSO for nebivolol, and KREBS for TAT-Gap19, L-NNA and GSNO). The average of all controls for each 'n' was set to a nominal value of '1' so that data is presented as a "fold change from control." For western blot analysis, each sample (guinea pig and human) was from a unique patient and was treated at an individual 'n,' and is represented by individual dots in figure 1.

For all experiments, t-test were unpaired and two-tailed. Normally distributed data were analyzed with a Welch's correction to account for variable SDs, while non-normal data were subjected to a Mann-Whitney test. Likewise, either an ordinary one-way ANOVA test was employed, or a Kruskal-Wallis test for non-parametric data, as appropriate. All error bars on graphs displayed as 95% CI. Samples were randomized, but not blinded, as inclusion/exclusion criteria and analysis parameters were established prior to experimentation and not subject to change. All data were analyzed using Prism (v. 8.4.3, Graphpad Software, San Diego, CA).

8. RESULTS

Cx43 Protein Expression in sPTL

A multitude of genes and proteins are differentially regulated in women who experience preterm labor(Paquette *et al.*, 2018; Knijnenburg *et al.*, 2019). We

JPET Fast Forward. Published on December 31, 2020 as DOI: 10.1124/jpet.120.000427
This article has not been copyedited and formatted. The final version may differ from this version.

previously determined that s-nitrosoglutathione reductase (GSNOR), a negative modulator of NO availability, is upregulated in sPTL myometrium, which decreases the availability of NO and reduces total protein S-nitrosations(Barnett *et al.*, 2018). Here we sought to determine if Cx43 is also dysregulated in sPTL myometrium. First, in order to establish a baseline of Cx43 expression throughout the entire gestational period (early, mid, late), something that cannot practically be done in women, we employed an animal model of preterm labor, the guinea pig. Data gathered from early gestation in the guinea pig allows us to better compare human preterm protein expression to a known standard. The guinea pig is preferred over other animal models, such as the mouse(Yellon *et al.*, 2009), because like humans, guinea pigs do not experience progesterone withdrawal prior to the onset of labor(Nnamani *et al.*, 2013).

In the guinea pig, when compared to non-pregnant (NP) myometrium (n=6), Cx43 expression was found to increase in early pregnancy (d15-30 - P=0.0025, n=7; Figure 1A, Supplemental Figure 1A) and remains elevated throughout (mid, d31-59 - P=0.0449, n=6; late, d60+ P=0.0373, n=6). Of interest, expression did not vary among early, mid and late pregnancy (ANOVA, p=0.9611). Based on the data provided by our animal model, we then analyzed human myometrial expression of Cx43 (Figure 1B, Supplemental Figure 1B). In human tissue we found a similar trend in which relative to NP myometrium (n=14), Cx43 expression was significantly higher in all pregnancy groups (PTNL P=0.0033, n=6, 32.0wk ± 2.32; TL P<0.0001, n=14, 39.0wk ± 0.44; TNL P<0.0001, n=14, 38.8wk ± 0.67), with the notable exception of sPTL (sPTL P=0.8411, n=6, 33.64wk ± 3.25). As with the guinea pig, there was also

JPET Fast Forward. Published on December 31, 2020 as DOI: 10.1124/jpet.120.000427
This article has not been copyedited and formatted. The final version may differ from this version.

no appreciable difference in expression of Cx43 in uncomplicated states of pregnancy (PTNL:TL:TNL, p=0.5190).

Effect of NO on Cx43 Phosphorylation & S-nitrosation

The expression of Cx43 in the myometrium is only one of several important metrics when establishing its role in contractile dynamics. It is well-known that Cx43's phosphorylation state, particularly at serine-368 (S368) on the c-terminus, is critical to GJC (contraction) function(Lampe *et al.*, 2000; Solan and Lampe, 2014). Because myometrium is known to relax to NO independent of the canonical cGMP-PKG pathway(Buxton, 2004), we sought to determine whether NO would facilitate an increase in Cx43 O-phosphorylation at S368 (pS368). Using an *ex vivo* organ bath, we attached human myometrial tissue strips to a force transducer in a physiological buffer, then exposed the tissue to either oxytocin (8 nM), after which it was snap-frozen with LN_2 (spray gun) at peak contraction, or to oxytocin, followed NO (GSNO, 300 μM), then snap-froze at maximal relaxation (TNL n=4, 3 samples per 'n'). Total protein lysate was extracted from the samples and the ratio of pS368:S368 was analyzed *via* western blot (Figure 2A, Supplemental Figure 2A). We found that the ratio of pS368:S368 was ~2.4-fold higher (P=0.0281) in myometrium treated with NO as compared to tissue treated with OT, intimating a role of NO in Cx43-mediated quiescence.

In addition to phosphorylation, we examined Cx43 S-nitrosation, a posttranslational modification that acts as a critical mediator of protein function in the myometrium. Total protein S-nitrosation in the myometrium can vary wildly based on

JPET Fast Forward. Published on December 31, 2020 as DOI: 10.1124/jpet.120.000427
This article has not been copyedited and formatted. The final version may differ from this version.

the pregnancy state, in particular in women who experience sPTL(Ulrich *et al.*, 2012). Moreover, this posttranslational modification is known to affect contractile dynamics(Barnett *et al.*, 2018). S-nitrosation of Cx43 has been shown in other tissue types to alter the protein's function(Retamal *et al.*, 2006; Lillo *et al.*, 2019); therefore, we sought to determine whether NO-mediated phosphorylation of Cx43 at S368 correlates with Cx-43 S-nitrosation. Using the same protein lysates as above, we performed a biotin switch assay to identify whether Cx43 was S-nitrosated when exposed to NO (300 µM). We found that SNO-Cx43 levels increased 2.08-fold in NO-treated samples (P=0.0046) over OT treated samples (Figure 2B, Supplemental Figure 2B), while total protein SNOs increased 1.37-fold (P=0.0274, Figure 2C, Supplemental Figure 2C).

Effect of NO on Cx43 HC Function

After determining that NO correlates to both an increase in the pS368:S368 ratio and Cx43 S-nitrosation, we next sought to determine whether NO would directly affect its function. This was accomplished through an ethidium bromide (EtBr) assay(Contreras *et al.*, 2003), which is measured as an increase in fluorescent signal as EtBr intercalates with nucleotides after passing though Cx43 HCs in the membrane. Telemorized pregnant human uterine smooth muscle cells (phUSMC), and HEK293 cells, which show no appreciable Cx43 expression (Figure 3D), were grown to ~50-80% confluence (n=3, ~3500 cells per well) and exposed to 10 µM EtBr for 5 minutes in Krebs-ringer buffer (-) Ca^{2+}. Following exposure, the experimental buffer was exchanged for fresh Krebs-ringer buffer (-) Ca^{2+} (t=0) and

JPET Fast Forward. Published on December 31, 2020 as DOI: 10.1124/jpet.120.000427
This article has not been copyedited and formatted. The final version may differ from this version.

placed in a 37°C incubator (95%:5%, O_2:CO_2). At each time point (t=0,30,60,90) treated cells were washed and fixed with paraformaldehyde to halt the reaction. Cells were then imaged at 4x and the relative fluorescent increase (normalized to total cell count by DAPI labeling) over t=0 was observed. A higher fluorescent signal infers a prolonged open-probability of the channel during the EtBr loading phase. Under baseline conditions relative fluorescent signal increased by 4.58-fold (± 0.734) at t=90 (P=0.0089, Figure 3A, 3C), which was completely eliminated by the use of 100 µM TAT-Gap19 (P=0.700), a membrane permeable inhibitor selective to the HC(Abudara *et al.*, 2014). The addition of NO (GSNO, 300 µM) increased the fluorescent signal by 3.36-fold (± 0.698) over t=0 (P=0.0365); however, at 90 min GSNO treatment did not increase the fluorescent signal above baseline conditions at 90 min (P=0.2963). To determine if this occurred because the assay was run in Ca^{2+}-free buffer, which facilitates an HC open-channel state(Li *et al.*, 1996), we evaluated the effect of physiological extracellular Ca^{2+} (2.5 mM), which closes the HC(Ek-Vitorín *et al.*, 2018). We found that the addition of NO (GSNO, 300 µM) significantly increased EtBr uptake over untreated baseline at 90 min (P=0.0119, Figure 3B). The fluorescent signal in HEK293 cells, which do not appreciably express Cx43 protein, was unchanged throughout the 90-minute observation period in both the untreated (ANOVA, P=0.8621) and NO-treated (ANOVA, P=0.2533) HEK293 cells (Figure 3A).

Cx43 HC inhibition and Tocolysis

JPET Fast Forward. Published on December 31, 2020 as DOI: 10.1124/jpet.120.000427
This article has not been copyedited and formatted. The final version may differ from this version.

It is well established that Cx43 is a critical facilitator of coordinated muscle contraction, so here we consider whether or not Cx43 inhibition exhibits useful tocolytic properties. Two Cx43 inhibitors were selected for their actions on the GJC and HC: (1) 18β-Glycyrrhetinic acid (18β-GA), a compound found in the roots of *Glycyrrhiza glabra L.* (black liquorice) that inhibits GJC and HC; and (2) TAT-Gap19, a HC-selective inhibitor consisting of a nine-amino acid peptide fragment from the Cx43 cytosolic loop which contains a TAT-modification (transactivating transcriptional activator from human immunodeficiency virus 1; Figure 4) that greatly increases cell permeability and action on the channel(Abudara *et al.*, 2014). Based on our previous data we posited that 18β-GA would blunt contractions by preventing the propagation of the contractile signal between uterine smooth muscle cells, while TAT-Gap19 would most likely confer positive inotropic effects by inhibiting normal HC function.

TAT-Gap19 was tested as a single dose at 100 μM (or buffer vol. equivalent) for 60 minutes in KCL-stimulated (60 mM, 3 minutes) tissue without the addition OT (n=3, 2 strips per patient). We hypothesized that TAT-Gap19 would promote a contractile state through HC-specific inhibition. Contractions from TNL myometrium that is not treated with OT will run down (data not shown); therefore, we were interested in determining if HC inhibition would promote contractions in tissue that would otherwise become quiescent. All TAT-Gap19 treated tissue maintained regular contractions throughout the dosing period (Figure 4A), while all but one control tissue ran down completely (contractions returned in all control samples following KCL-stimulation after 60-minute dosing period). Both AUC ($P<0.0001$) and

JPET Fast Forward. Published on December 31, 2020 as DOI: 10.1124/jpet.120.000427
This article has not been copyedited and formatted. The final version may differ from this version.

peak tension (P=0.005) were significantly higher in TAT-Gap19 treated tissue (Figure 4B).

Co-administration of a Cx43 GJC Inhibitor and eNOS activator

A primary concern when administering any tocolytic are the potential off-target effects on the fetus and mother. Fetal toxicity not only limits which drugs may be used, but also at which concentrations. Because of this we propose that the co-administration of two or more drugs at modest doses may provide a complementary effect, particularly when each drug targets a known pathway associated with sPTL. We previously generated a limited data set in which nebivolol, an eNOS activator, displayed tocolytic properties(Barnett and Buxton, 2018). Here we expanded upon that investigation and sought to establish whether or not the co-administration of nebivolol and 18β-GA, an Cx43 inhibitor, exerts enhanced negative inotropic effects.

To begin, we experimentally derived IC_{50} values for nebivolol (Figure 5A) and 18β-GA (Figure 5B) using TNL myometrium (log_{drug} vs. response) with the organ bath technique described above. We determined that the IC_{50} for nebivolol, based on AUC, was 8.26 μM (n=3 patients), while 18β-GA 102 μM (n=5 patients). Because nebivolol acts on endothelial beta-3 adrenergic receptors (β3-AR) to produce NO through eNOS activation(Reidenbach *et al.*, 2007), and potentially on β3-ARs located on uterine myocytes, we also tested the effects of L-NNA (100μM, 20 minutes pre-incubation), a potent inhibitor of eNOS activity, on TNL tissue treated with 10μM nebivolol (n=3 patients per condition, 1-3 myometrial strips per patient), and found that nebivolol did not significantly decrease AUC in the presence of L-

JPET Fast Forward. Published on December 31, 2020 as DOI: 10.1124/jpet.120.000427
This article has not been copyedited and formatted. The final version may differ from this version.

NNA (p=0.1405, data not shown), suggesting that nebivolol's action on the myometrium rests primarily on NO production.

To test the effects of combination tocolytics, we first independently dosed TNL tissue (n=3 patients per condition, 1-3 myometrial strips per patient) at the approximate IC_{50} for nebivolol (10 μM) and 18β-GA (100 μM, Figure 6C). Roughly in line with our experimentally derived IC_{50} data, the AUC for nebivolol dropped to 49.9% (± 6.7) of control (P<0.0001), with 18β-GA at 33.8% (± 7.2) (P<0.0001), of which there was not a significant difference of AUCs between nebivolol and 18β-GA at their respective IC_{50} values (P=0.1506, Figure 6A). Similarly, the peak tension after nebivolol IC_{50} administration decreased to 72.9% (± 6.5 SEM) of control (P<0.0001), an 18β-GA to 33.8% (± 7.2) (P<0.0001, Figure 6B).

When nebivolol and 18β-GA were co-administered for 1 hour (10 μM, 100 μM respectively), their effects on AUC and peak force were additive. AUC dropped to 12.5% (± 2.5) of control (p<0.0001), which was an additional 37.4% decrease over nebivolol alone (P=0.0061), and an additional 21.3% decrease over 18β-GA (P=0.0088, Figure 6A). Co-administration also decreased peak tension to 21.4% (± 4.8) over control (p<0.0001), which constituted a 51.1% (P=0.009) and 19.3% (P=0.0396) drop in peak tension, relative to their IC_{50} values, with nebivolol and 18β-GA, respectively (Figure 6B), and can be seen visually in the representative traces (Figure 6C).

9. DISCUSSION

JPET Fast Forward. Published on December 31, 2020 as DOI: 10.1124/jpet.120.000427
This article has not been copyedited and formatted. The final version may differ from this version.

Preterm birth remains the single greatest cause of neonatal morbidity and hospitalization following pregnancy(Miniño *et al.*, 2006; Rundell and Panchal, 2017; Granese *et al.*, 2019). The preterm birth rate in the US and the UK has hovered between 8-12% for decades, resulting in 20,000 infant deaths annually in the US alone(Martin *et al.*, 2013). Novel tocolytic development will benefit from embracing the specific disparities found in women who experience sPTL in lieu of the 'borrowed pharmacology' currently favored. For this reason, we sought to investigate the regulation and modulation of the important myometrial CAP protein, Cx43.

Connexins are ubiquitously expressed in most cell types(Söhl and Willecke, 2004). Cx43 is integral to muscle function where its dysregulation can be consequential(Ai *et al.*, 2000; He and Chen, 2016). While data surrounding the expression of Cx43, *per se*, does not provide resolution concerning its conformation (GJC vs. HC vs. trafficking), it does afford information regarding the myocyte's state and tissue phenotype. Our animal model predicted that Cx43 expression should increase early in pregnancy and remain elevated throughout gestation (Figure 1A). In human myometrium our Cx43 expression data is consistent with our animal model (Figure 1B), as well as with data from other laboratories(Pierce *et al.*, 2002). Of interest, we did not observe differential expression of Cx43 after onset of labor (TNL vs. TL), nor in preterm tissue as compared to term (PTNL vs TNL). Importantly, Cx43 expression was significantly higher in all pregnancy states, relative to NP, with the notable exception sPTL, where Cx43 expression was on par with NP. Similar Cx43 dysregulation in other reproductive tissues during pregnancy affects birth timing; for instance, Cx43 has been found to be downregulated in 1st trimester villi

JPET Fast Forward. Published on December 31, 2020 as DOI: 10.1124/jpet.120.000427
This article has not been copyedited and formatted. The final version may differ from this version.

and decidua of women who experience recurrent pregnancy loss(He and Chen, 2016). Further, Wnt-1 activation is known to increase expression of Cx43 in myocytes(Ai *et al.*, 2000), and it has been shown that *WNT1* is downregulated in the fetal membrane of women who experience PTL(Pereyra *et al.*, 2018). As such, our data further correlates Cx43 dysregulation to aberrant labor, and due to Cx43's integral role as a smooth muscle CAP protein, this dysregulation suggest that Cx43 may be a unique target of interest for tocolytic development.

Beyond Cx43 protein expression, the posttranslational state of Cx43 is fundamental to its function. In particular, phosphorylation of S368 is of keen interest as this posttranslational modification decreases GJC conductance(Lampe *et al.*, 2000) and facilitates its internalization(Boswell-casteel *et al.*, 2016; Ribeiro-Rodrigues *et al.*, 2017; Ek-Vitorín *et al.*, 2018). Our finding that NO increases the ratio of pS368 in myometrium (Figure 2A) is significant in that it bolsters a growing body of evidence that confirms our previous data demonstrating NO-mediated cGMP-independent relaxation of the human myometrium(Bradley *et al.*, 1998). In addition to altering its phosphorylation state, we also determined that that Cx43 is directly S-nitrosated by NO during relaxation of the myometrium (Figure 2B), which has been shown to alter conformation and conductance of the channel(Retamal *et al.*, 2006; Straub *et al.*, 2011; Dimitrova *et al.*, 2017). Together, these data provide compelling evidence that NO's action on Cx43 serves as an important mediator of relaxation in the myometrium.

Based on our results, we elected to investigate the effect of NO on HC function. The HC is associated with quiescence in that it permeates PGE_2(Burra and Jiang,

2009) and other small molecular weight mediators, including ATP(King and Lampe, 2005), into the extracellular space. Cx43-SNO-C271 has been shown to activate both the HC(Contreras *et al.*, 2003) and the GJC(Straub *et al.*, 2011) at the myoendothelial junction. In line with these finding, our data indicate that NO activates the HC in human uterine smooth muscle cells under physiological extracellular Ca^{2+}, and this activation is blocked with the addition of an HC-selective inhibitor, TAT-Gap19 (Figure 3). Our finding that the HC open-state is correlated to the presence of NO provides additional data in support of the non-canonical relaxation of the myometrium by NO. Whether HC activation is critically mediated by SNO-Cx43 formation, or pS368-Cx43 formation, or both, awaits future investigation.

The effect of NO on the biochemical state of Cx43 in the myometrium is compelling; however, simply modulating Cx43's SNO or O-phosphorylation state does not guarantee tocolysis in myometrial tissue. For this reason, we sought to determine whether pharmacological mediation of Cx43 and NO exhibits novel tocolytic properties. To this end, we first independently overserved the effects HC and GJC inhibition on myometrial contractile dynamics. As we hypothesized, the inhibition of the HC with TAT-Gap19 conveyed positive inotropic effect on the myometrium (Figure 4), further reinforcing the concept that the HC is critical to the maintenance of myometrial quiescence. Conversely, the inhibition of Cx43 with 18β-GA, which also promotes Cx43-pS368 formation(Liang *et al.*, 2008), blunted contractile dynamics (AUC) in a dose-depend manner (Figure 5B). Taken together, these data indicate that activation of the HC and inhibition of GJC may function in concert to mediate quiescence.

JPET Fast Forward. Published on December 31, 2020 as DOI: 10.1124/jpet.120.000427
This article has not been copyedited and formatted. The final version may differ from this version.

With the therapeutic potential of GJC inhibition established, we posited that increasing endogenous NO-availability would further enhance tocolysis by promoting Cx43 S-nitrosation and Serine O-phosphorylation (pS368) to increase HC activity and blunt that of the GJC. We have previously demonstrated, in an limited manner, that NO generation through eNOS activation (nebivolol, Bystolic™, Allergan)(Barnett and Buxton, 2018) exhibits a tocolytic effect. Here we expanded upon that finding and determined that nebivolol conveys robust negative inotropic effects on the myometrium in a dose-dependent manner (Figure 5A). Interestingly, because nebivolol is an agonist of β3-ARs, we must consider that some of the effects of the drug may be the result of β3-AR activation directly on uterine myocytes, rather than solely on β3-AR-mediated eNOS activation on the endothelium. In previously published work we determined that the β3-AR antagonist, SR59230A, reduced the action of nebivolol by ~50%(Barnett and Buxton, 2018), and here we found that in the presence L-NNA, an eNOS antagonist, nebivolol administered at its IC_{50} dose (10 μM) does not significantly reduce AUC. While the activation of β3-ARs on uterine myocytes may in fact play a role in myometrial quiescence, here we show that nebivolol's actions on myometrial tissue are largely the result of NO generation. These data support the notion that GJC Inhibition and protein S-nitrosation are fundamental drivers of myometrial quiescence.

A significant real-world problem when administering tocolytics is the effect on the fetus. The necessary high-doses needed to blunt preterm labor with drugs like $MgSO_4$, terbutaline, or nifedipine can affect fetal heart rate(Verdurmen *et al.*, 2017), and a drug specifically designed as a tocolytic, atosiban, an OXTR-antagonist, is not

effective at delaying PTB at any dose(Flenady *et al.*, 2014). Taken together, this presents an interesting pharmacologic conundrum. We believe that the solution may lie in the co-administration of multiple tocolytics at low doses. Not only might this put less stress on the fetus by limiting its exposure to the drugs, but we also suggest that by targeting multiple dysregulated pathways the potential to halt PTL and delay PTB increases significantly. This concept is not entirely novel. Clinical trials with the co-administration of various beta-adrenergic receptor modulators, such as ritodrine, in combination with other drugs [indomethacin (COX-1/2), MgSO4 (VDCC)] were carried out, with no clear benefit(Vogel *et al.*, 2014). These findings are not particularly surprising considering the limited role cyclic nucleotides play specifically in myometrial quiescence. Our approach differs in that we are targeting proteins and pathways known to be dysregulated in women who experience preterm labor. Not only is Cx43 dysregulated in sPTL myometrium (Figure 1B), but we have previously shown that total protein S-nitrosations in the myometrium are decreased due to the overexpression of GSNOR, an catabolic degrader of NO, in sPTL myometrium(Barnett *et al.*, 2018). It is for these reasons that we elected to co-administer 18β-GA and nebivolol at their IC_{50} values and found that the combined effect on AUC and peak tension was synergistic, all but abolishing contractions (Figures 5 and 6). Further studies must be conducted to determine if the tocolytic properties of 18β-GA and nebivolol fully transfer to sPTL myometrium. This is a reasonable concern as the upregulation GSNOR is sPTL myometrium may subdue the tocolytic benefits of nebivolol-mediated NO generation, and the downregulation of Cx43 in sPTL may further reduce the negative inotropic actions of 18β-GA.

JPET Fast Forward. Published on December 31, 2020 as DOI: 10.1124/jpet.120.000427
This article has not been copyedited and formatted. The final version may differ from this version.

While the solution to the problem that is sPTL continues to elude the scientific community, there is little doubt that to decipher this mystery we must better understand dysregulated pathways during affected pregnancies, and in turn develop novel therapeutics that mitigate these disparities. Cx43 is a foundational CAP protein in the myometrium, and here we show that it is dysregulated in sPTL myometrium and its function is moderated by NO. By inhibiting GJC activity, and increasing endogenous NO-availability, we were able to severely blunt contractions, reinforcing the concept that pharmacologic intervention of multiple dysregulated pathways during pregnancy enhances quiescence. Additional biochemical and genetic pathways associated with sPTL are being recognized with increased frequency, and with this comes the potential for identifying new and effective tocolytics.

10. ACKNOWLEDGEMENTS

The authors would like to acknowledge Veronica Arinze for cell culture, Amy Savignac and Veronica Arinze for human tissue collection, and Coral Gramelspacher, Jennifer Burnham, and Irene Richardson for laboratory assistance. The authors would also like to thank the patients, physicians and nurses of Renown® Health OBGYN for their support of our research.

11. AUTHOR CONTRIBUTIONS

Participated in research design: Barnett, Buxton

Conducted Experiments: Barnett, Buxton, Asif, Anderson

Performed data analysis: Barnett, Buxton, Asif

Wrote or contributed to writing: Barnett, Buxton

No author has an actual or perceived conflict of interest with the contents of this article.

JPET Fast Forward. Published on December 31, 2020 as DOI: 10.1124/jpet.120.000427
This article has not been copyedited and formatted. The final version may differ from this version.

12. REFERENCES

Abudara V, Bechberger J, Freitas-Andrade M, De Bock M, Wang N, Bultynck G, Naus CC, Leybaert L, and Giaume C (2014) The connexin43 mimetic peptide Gap19 inhibits hemichannels without altering gap junctional communication in astrocytes. *Front Cell Neurosci* **8**:1–8.

Ai Z, Fischer A, Spray DC, Brown AMC, and Fishman GI (2000) Wnt-1 regulation of connexin43 in cardiac myocytes. *J Clin Invest* **105**:161–171.

Barnett SD, and Buxton ILO (2018) Hiding in Plain Sight: Nebivolol Exhibits Compelling Tocolytic Properties. *J Cell Mol Med* **22**:6391–6395.

Barnett SD, and Buxton ILO (2017) The role of S-nitrosoglutathione reductase (GSNOR) in human disease and therapy. *Crit Rev Biochem Mol Biol* **52**.

Barnett SD, Smith CR, Ulrich CC, Baker JE, and Buxton ILO (2018) S-Nitrosoglutathione Reductase Underlies the Dysfunctional Relaxation to Nitric Oxide in Preterm Labor. *Sci Rep* **8**:1–12, Springer US.

Behrman RE, and Butler AS (2007) *Preterm birth: Causes, Consequences, and prevention*.

Boswell-casteel RC, Johnson JM, Duggan KD, Tsutsui Y, and Hays FA (2016) Selectivity of Cx43 channels is regulated through PKC-dependent phosphorylation. *Circ Res* **98**:57–65.

Bradley KK, Buxton ILOL, Barber JE, McGaw T, and Bradley ME (1998) Nitric oxide relaxes human myometrium by a cGMP-independent mechanism. *Am J Physiol* **275**:C1668-73.

Burra S, and Jiang JX (2009) Connexin 43 hemichannel opening associated with

Prostaglandin E2 release is adaptively regulated by mechanical stimulation. *Commun Integr Biol* **2**:239–240.

Buxton IL (2004) Regulation of uterine function: a biochemical conundrum in the regulation of smooth muscle relaxation. *Mol Pharmacol* **65**:1051–1059.

Contreras JE, Saez JC, Bukauskas FF, and Bennett MVL (2003) Gating and regulation of connexin 43 (Cx43) hemichannels. *Proc Natl Acad Sci* **100**:11388–11393.

Dimitrova N, Zamudio JR, Jong RM, Soukup D, Resnick R, Sarma K, Ward AJ, Raj A, Lee J, Sharp PA, and Jacks T (2017) Compartmentalized Connexin 43 S-Nitrosylation/Denitrosylation Regulates Heterocellular Communication in the Vessel Wall. *PLoS One* **32**:736–740.

Ek-Vitorín JF, Pontifex TK, and Burt JM (2018) Cx43 channel gating and permeation: Multiple phosphorylation-dependent roles of the carboxyl terminus. *Int J Mol Sci* **19**:1–19.

Flenady V, Reinebrant HE, Liley HG, Tambimuttu EG, and Papatsonis DNM (2014) Oxytocin receptor antagonists for inhibiting preterm labour. *Cochrane Database Syst Rev* **2014**.

Foster MW, McMahon TJ, and Stamler JS (2003) S-nitrosylation in health and disease. *Trends Mol Med* **9**:160–168.

Granese R, Gitto E, D'Angelo G, Falsaperla R, Corsello G, Amadore D, Calagna G, Fazzolari I, Grasso R, and Triolo O (2019) Preterm birth: Seven-year retrospective study in a single centre population. *Ital J Pediatr* **45**:1–6, Italian Journal of Pediatrics.

Hansen DB, Braunstein TH, Nielsen MS, and Macaulay N (2014) Distinct permeation

profiles of the connexin 30 and 43 hemichannels. *FEBS Lett* **588**:1446–1457, Federation of European Biochemical Societies.

He X, and Chen Q (2016) Reduced expressions of connexin 43 and VEGF in the first-trimester tissues from women with recurrent pregnancy loss. *Reprod Biol Endocrinol* **14**:1–7, Reproductive Biology and Endocrinology.

Heyman NS, Cowles CL, Barnett SD, Wu YY, Cullison C, Singer CA, Leblanc N, and Buxton ILO (2013) TREK-1 currents in smooth muscle cells from pregnant human myometrium. *Am J Physiol - Cell Physiol* **305**:632–642.

Jaffrey SR, and Snyder SH (2001) The Biotin Switch Method for the Detection of S-Nitrosylated Proteins. *Sci Signal* **2001**:pl1--pl1, Science Signaling.

King TJ, and Lampe PD (2005) Temporal regulation of connexin phosphorylation in embryonic and adult tissues. *Biochim Biophys Acta - Biomembr* **1719**:24–35.

Knijnenburg TA, Vockley JG, Chambwe N, Gibbs DL, Humphries C, Huddleston KC, Klein E, Kothiyal P, Tasseff R, Dhankani V, Bodian DL, Wong WSW, Glusman G, Mauldin DE, Miller M, Slagel J, Elasady S, Roach JC, Kramer R, Leinonen K, Linthorst J, Baveja R, Baker R, Solomon BD, Eley G, Iyer RK, Maxwell GL, Bernard B, Shmulevich I, Hood L, and Niederhuber JE (2019) Genomic and molecular characterization of preterm birth. *Proc Natl Acad Sci U S A* **116**:5819–5827.

Lai PF, Tribe RM, and Johnson MR (2016) Differential impact of acute and prolonged cAMP agonist exposure on protein kinase A activation and human myometrium contractile activity. *J Physiol* **594**:6369–6393.

Lampe PD, TenBroek EM, Burt JM, Kurata WE, Johnson RG, and Lau AF (2000) Phosphorylation of connexin43 on serine368 by protein kinase C regulates gap

junctional communication. *J Cell Biol* **149**:1503–1512.

Leithe E, Mesnil M, and Aasen T (2018) The connexin 43 C-terminus: A tail of many tales. *Biochim Biophys Acta - Biomembr* **1860**:48–64, Elsevier B.V.

Li H, Liu TF, Lazrak A, Peracchia C, Goldberg GS, Lampe PD, and Johnson RG (1996) Properties and regulation of gap junctional hemichannels in the plasma membranes of cultured cells. *J Cell Biol* **134**:1019–1030.

Liang JY, Wang SM, Chung TH, Yang SH, and Wu JC (2008) Effects of 18-glycyrrhetinic acid on serine 368 phosphorylation of connexin43 in rat neonatal cardiomyocytes. *Cell Biol Int* **32**:1371–1379, Elsevier Ltd.

Lillo MA, Himelman E, Shirokova N, Xie LH, Fraidenraich D, and Contreras JE (2019) S-nitrosylation of connexin43 hemichannels elicits cardiac stress–induced arrhythmias in Duchenne muscular dystrophy mice. *JCI Insight* **4**.

Martin JA, Hamilton BE, Ventura SJ, Osterman MJK, and Mathews TJ (2013) Births: final data for 2011. *CDC*.

Miniño AM, Heron MP, and Smith BL (2006) Deaths: preliminary data for 2004. *Natl Vital Stat Rep* **54**:1–49.

Nnamani MC, Plaza S, Romero R, and Wagner GP (2013) Evidence for independent evolution of functional progesterone withdrawal in primates and guinea pigs. *Evol Med Public Heal* **2013**:273–288.

Paquette AG, Shynlova O, Kibschull M, Price ND, and Lye SJ (2018) Comparative analysis of gene expression in maternal peripheral blood and monocytes during spontaneous preterm labor. *Am J Obstet Gynecol* **218**:345.e1-345.e30, Elsevier Inc.

Pereyra S, Sosa C, Bertoni B, and Sapiro R (2018) Transcriptomic analysis of fetal membranes reveals pathways involved in preterm birth. *bioRxiv* 1–14, BMC Medical Genomics.

Pierce BT, Calhoun BC, Adolphson KR, Lau AF, and Pierce LM (2002) Connexin 43 expression in normal versus dysfunctional labor. *Am J Obstet Gynecol* **186**:504–11.

Reidenbach C, Schwinger RHG, Steinritz D, Kehe K, Thiermann H, Klotz T, Sommer F, Bloch W, and Brixius K (2007) Nebivolol induces eNOS activation and NO-liberation in murine corpus cavernosum. *Life Sci* **80**:2421–2427.

Retamal MA, Cortés CJ, Reuss L, Bennett MVL, and Sáez JC (2006) S-nitrosylation and permeation through connexin 43 hemichannels in astrocytes: Induction by oxidant stress and reversal by reducing agents. *Proc Natl Acad Sci U S A* **103**:4475–4480.

Ribeiro-Rodrigues TM, Martins-Marques T, Morel S, Kwak BR, and Girão H (2017) Role of connexin 43 in different forms of intercellular communication – gap junctions, extracellular vesicles and tunnelling nanotubes. *J Cell Sci* **130**:3619–3630.

Rundell K, and Panchal B (2017) Preterm labor: prevention and management. *Am Fam Physician* **95**:366–372.

Söhl G, and Willecke K (2004) Gap junctions and the connexin protein family. *Cardiovasc Res* **62**:228–232.

Solan JL, and Lampe PD (2014) Specific Cx43 phosphorylation events regulate gap junction turnover in vivo. *FEBS Lett* **588**:1423–9.

Straub AC, Billaud M, Johnstone SR, Best AK, Yemen S, Dwyer ST, Looft-Wilson R, Lysiak JJ, Gaston B, Palmer L, and Isakson BE (2011) Compartmentalized

connexin 43 S-nitrosylation/denitrosylation regulates heterocellular communication in the vessel wall. *Arterioscler Thromb Vasc Biol* **31**:399–407.

Ulrich C, Quillici DR, Schegg K, Woolsey R, Nordmeier A, and Buxton ILO (2012) Uterine Smooth Muscle S-Nitrosylproteome in Pregnancy. *Mol Pharmacol* **81**:143–153.

Vanbésien O, and Eichner E (1956) Relaxin. *Br Med J* **2**:1171.

Verdurmen KMJ, Hulsenboom ADJ, van Laar JOEH, and Oei SG (2017) Effect of tocolytic drugs on fetal heart rate variability: a systematic review. *J Matern Neonatal Med* **30**:2387–2394, Taylor & Francis.

Vogel JP, Nardin JM, Dowswell T, West HM, and Oladapo OT (2014) Combination of tocolytic agents for inhibiting preterm labour. *Cochrane Database Syst Rev* **2014**.

WHO (2015) WHO recommendation on the use of tocolytic treatment for inhibiting preterm labour. 1–13.

Yellon SM, Burns AE, See JL, Lechuga TJ, and Kirby MA (2009) Progesterone withdrawal promotes remodeling processes in the nonpregnant mouse cervix. *Biol Reprod* **81**:1–6.

13. FOOTNOTES

a) Funding Information

This work was supported by the National Institutes of Health [R01 grant HD091114] awarded to Iain L.O. Buxton.

JPET Fast Forward. Published on December 31, 2020 as DOI: 10.1124/jpet.120.000427
This article has not been copyedited and formatted. The final version may differ from this version.

14. Figure Legends

Figure 1: Cx43 is dysregulated in sPTL myometrium - (a) Myometrial Cx43 expression in guinea pig increases ~ 2-fold in early pregnancy (d15-30, P=0.0025) and does not change significantly throughout the ~72d gestation period (early:mid:late, p=0.9611). (b) Similarly, human myometrial expression of Cx43 increases by ~ 2.5-fold in PTNL tissue (P=0.0033) and holds steady to term (TL P<0.0001, TNL P<0.0001); however, sPTL myometrial expression of Cx43 is not significantly different than NP tissue (P=0.8411), implying a dysregulation of its expression.

Figure 2: Cx43 S-nitrosation promotes GJC inhibition (Cx43-pS368) in human myometrium - Human myometrial tissue (TNL) was hung in an organ bath and exposed to either oxytocin (OT) or nitric oxide (NO). (a) the ratio of pS368, a posttranslational modification that promotes GJC inhibition (quiescence) was ~2.4-fold higher in NO-treated tissue (P=0.0281), (b) which also correlated to an ~2-fold increase in Cx43 S-nitrosation (P=0.0046). (c) Total protein S-nitrosation in the tissue lysate also increased by ~1.4-fold over OT-treated tissue (P=0.0274).

Figure 3: Nitric oxide promotes Cx43 HC open-state: Ethidium bromide (EtBr) selectively permeates Cx43 channels. (a,b) human myometrial or HEK293 cells were exposed EtBr ± GSNO or TAT-Gap19 (HC blocker) in a Ca^{2+}-free buffer for 5 minutes, then washed out. (a) Under baseline conditions (P=0.0089) and with GSNO (P=0.0365),

EtBr uptake through HCs was significantly higher by 90 minutes in myometrial cells, but not in those exposed to TAT-Gap19 (P=0.700), while no appreciable uptake of EtBr was observed in HEK293 cells (+) GSNO (P=0.2533) or (-) GSNO (P=0.8621). (b) Under 2.5 mM Ca^{2+}, which increases the closed-state probability of Cx43, fluorescent signal in myometrial cells exposed to GSNO increased significantly over baseline treatment at 90 minutes (P=0.0119). (c) 300x300 pixel magnification of 4x acquired images represented in panel (a) at t=0 and t=90, where cellular nuclei are false colored blue (DAPI), and EtBr green (Cx43). (dd) western blot data depicting the absence of Cx43 in HEK293 cells.

Figure 4: Cx43 HC inhibition promotes myometrial contractions: Human myometrial tissue (TNL, n=4) were KCL-challenged (60mM, 3 minutes) in an organ bath to initiate contractions, but were not exposed to oxytocin. (a) Tissue treated with TAT-Gap19 (100µM), a Cx43 HC-selective inhibitor) maintained contractions throughout the experimental period, while control tissue lost all contraction by ~100 minutes (contraction returned upon second KCL challenge after washout). (b) In the control tissue AUC decreased by ~80% as compared to TAT-Gap19-treated tissue (P<0.0001) and peak tension falling ~69% (P=0.005). (c) TAT-Gap19 consist of a 9-amino acid cytosolic loop fragment of Cx43, and a linked N-terminal ‘transactivator of transcription’ (TAT) modifier which increases membrane permeability and enhances its inhibitory effect.

JPET Fast Forward. Published on December 31, 2020 as DOI: 10.1124/jpet.120.000427
This article has not been copyedited and formatted. The final version may differ from this version.

Figure 5: Myometrial IC_{50} values of nebivolol and 18β-Glycyrrhetinic acid - Nebivolol is known to increase the generation of nitric oxide through eNOS activation, while 18β-GA blocks Cx43 GJCs. TNL myometrium was hung in an organ bath and exposed to either (a) 1,3,10,30 or 100μM nebivolol (n=3), or (b) 3,10,30,100 or 300μM 18β-GA (n=5) for one hour. Calculated IC_{50} values are based on the AUC of the last three contractions of the dosing period prior to washout, and were 8.13μM and 102μM, for nebivolol and 18β-GA, respectively.

Figure 6: Co-administration of nebivolol and 18β-Glycyrrhetinic acid impart a synergistic negative inotropic effect - TNL myometrium (n=3 per condition) was hung in an organ bath and exposed to either nebivolol (10 μM), 18β-GA (100 μ), or a combination of both (10 μM, 100 μM). (a) Relative to control there was a significant decrease in AUC for individual and combined doses (####, P<0.0001, t-test between control and each dosing scheme), and the co-administration of nebivolol and 18β-GA decreased the AUC to 12.5% (± 2.5) of control (p<0.0001), which represents a 37.4% further decrease over nebivolol alone (P=0.0061), and an additional 21.3% decrease over 18β-GA alone (P=0.0088). (b) Similarly, relative to control there was a significant decrease in 'peak force' for individual and combined doses (####, P<0.0001, t-test between control and each dosing scheme), and the co-administration of nebivolol and 18β-GA decreased peak tension to 21.4% (± 4.8) over control (p<0.0001), which constituted a 51.1% (nebivolol, P=0.009) and 19.3% (18β-GA, P=0.0396) drop in peak tension, relative to their IC_{50} doses. (c) Relative change in tension after IC_{50} administration of '18β-GA' (top

JPET Fast Forward. Published on December 31, 2020 as DOI: 10.1124/jpet.120.000427
This article has not been copyedited and formatted. The final version may differ from this version.

panel), ‘nebivolol’ (middle panel), or ‘both’ (bottom panel) in TNL myometrium. Drug dosing represented in blue (—) and control tissue in grey (—).

JPET Fast Forward. Published on December 31, 2020 as DOI: 10.1124/jpet.120.000427
This article has not been copyedited and formatted. The final version may differ from this version.

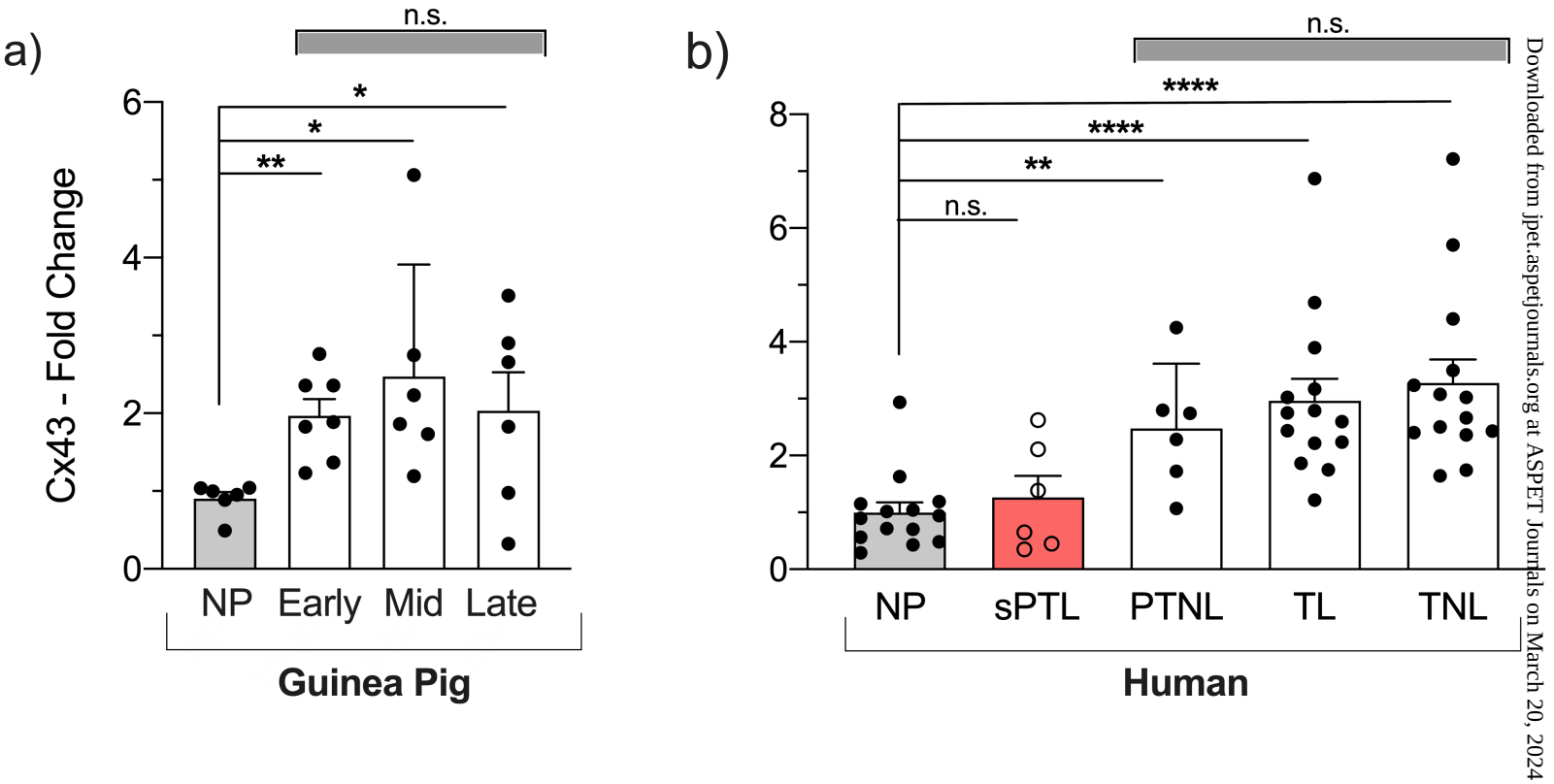

Figure 1

JPET Fast Forward. Published on December 31, 2020 as DOI: 10.1124/jpet.120.000427
This article has not been copyedited and formatted. The final version may differ from this version.

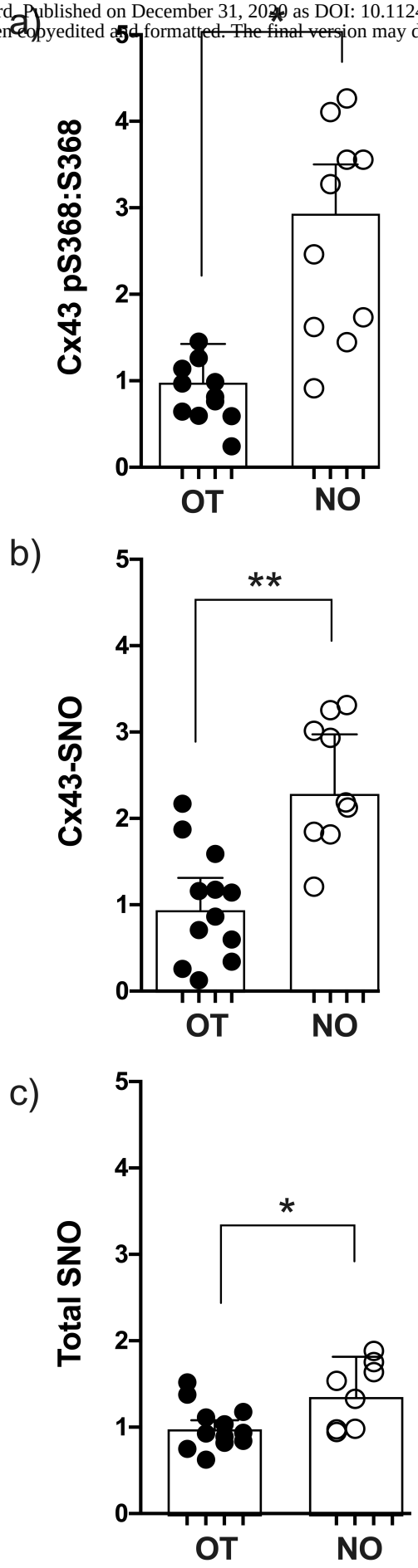

Figure 2

JPET Fast Forward. Published on December 31, 2020 as DOI: 10.1124/jpet.120.000427
This article has not been copyedited and formatted. The final version may differ from this version.

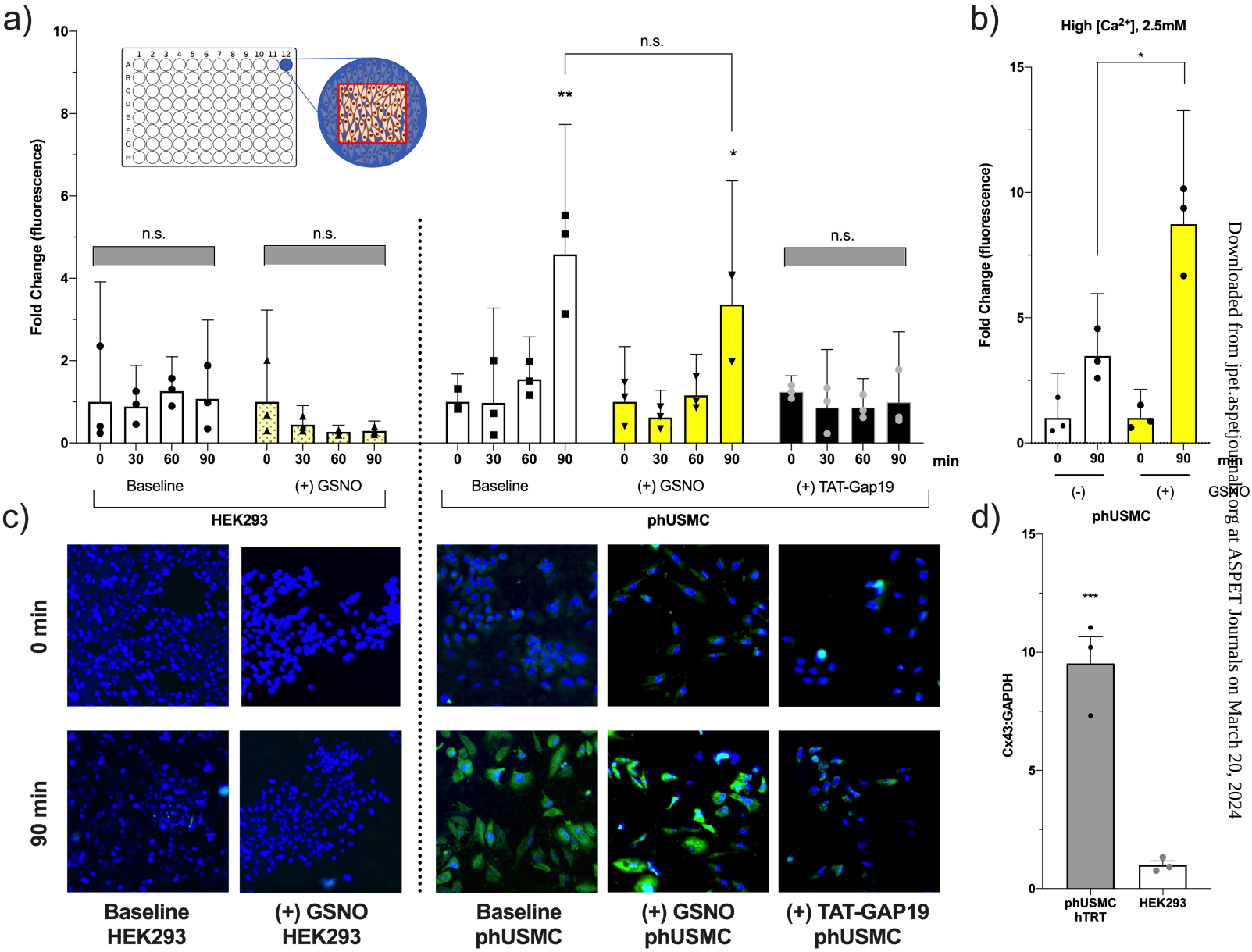

Figure 3

JPET Fast Forward. Published on December 31, 2020 as DOI: 10.1124/jpet.120.000427
This article has not been copyedited and formatted. The final version may differ from this version.

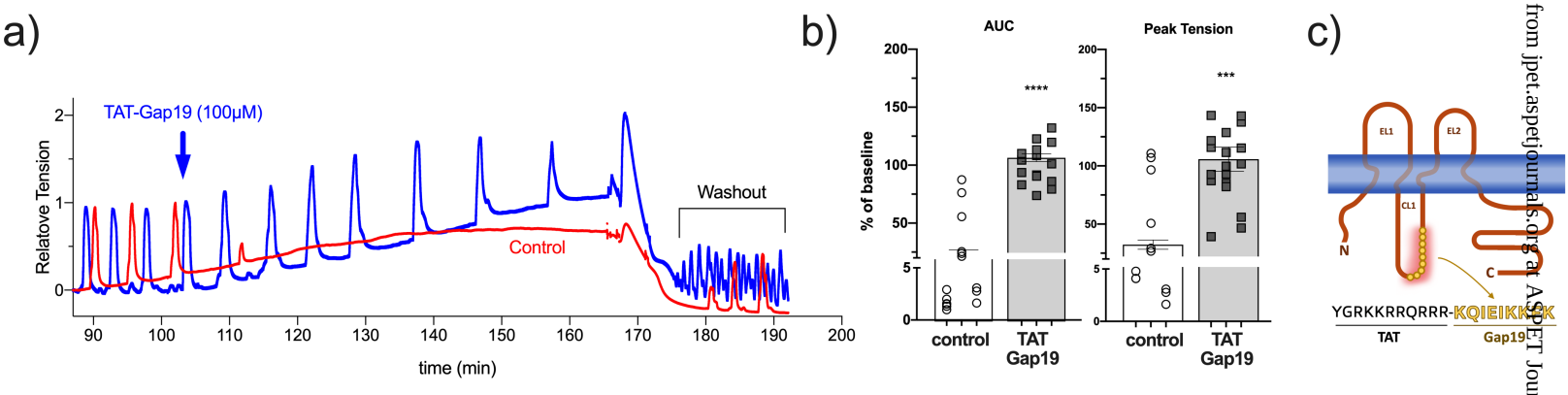

Figure 4

JPET Fast Forward. Published on December 31, 2020 as DOI: 10.1124/jpet.120.000427
This article has not been copyedited and formatted. The final version may differ from this version.

a)

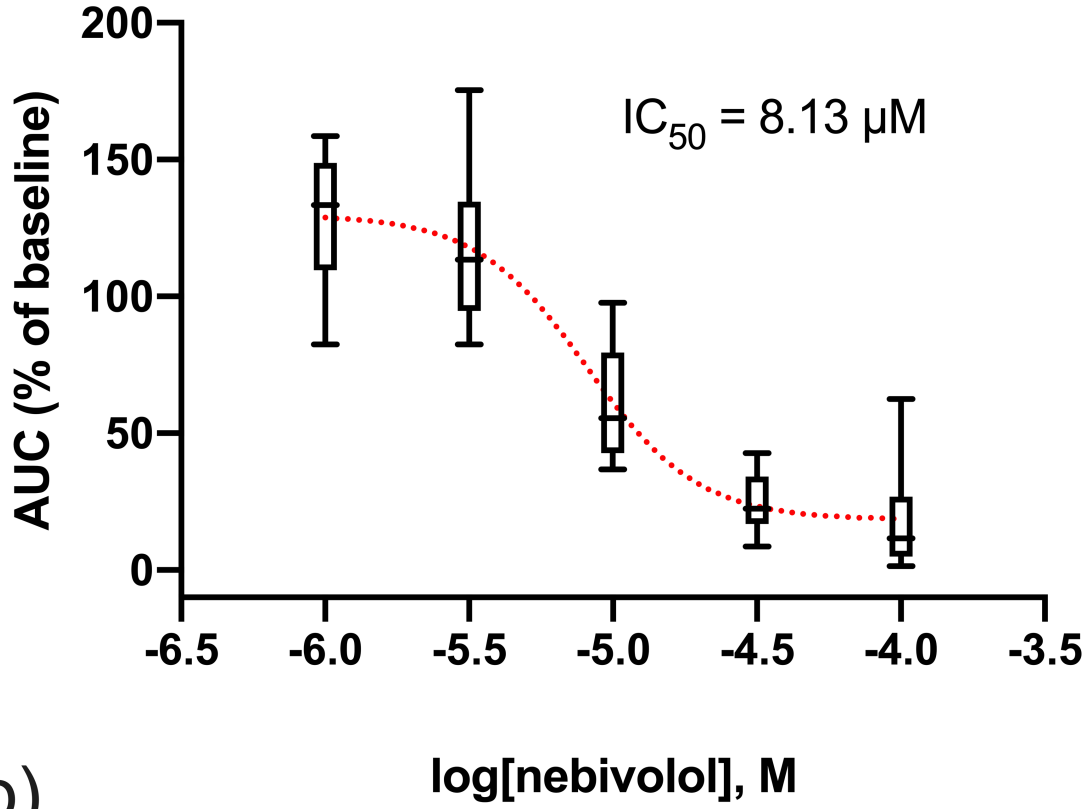

b)

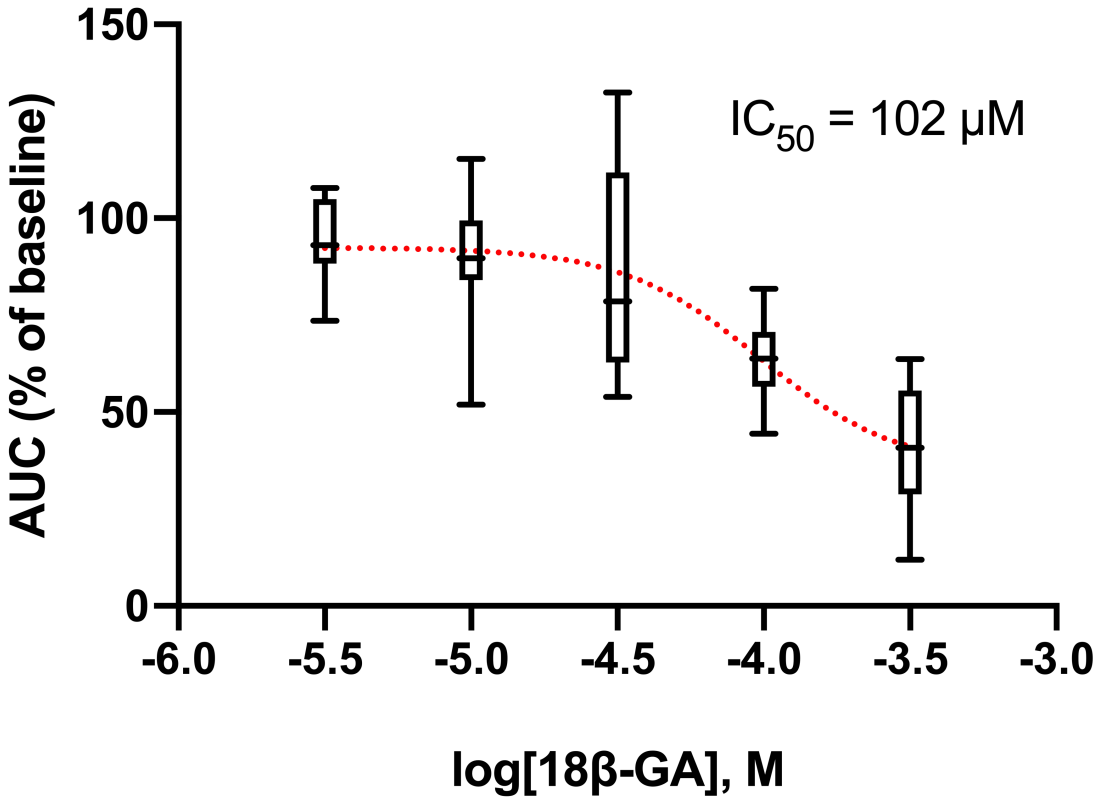

Figure 5

JPET Fast Forward. Published on December 31, 2020 as DOI: 10.1124/jpet.120.000427
This article has not been copyedited and formatted. The final version may differ from this version.

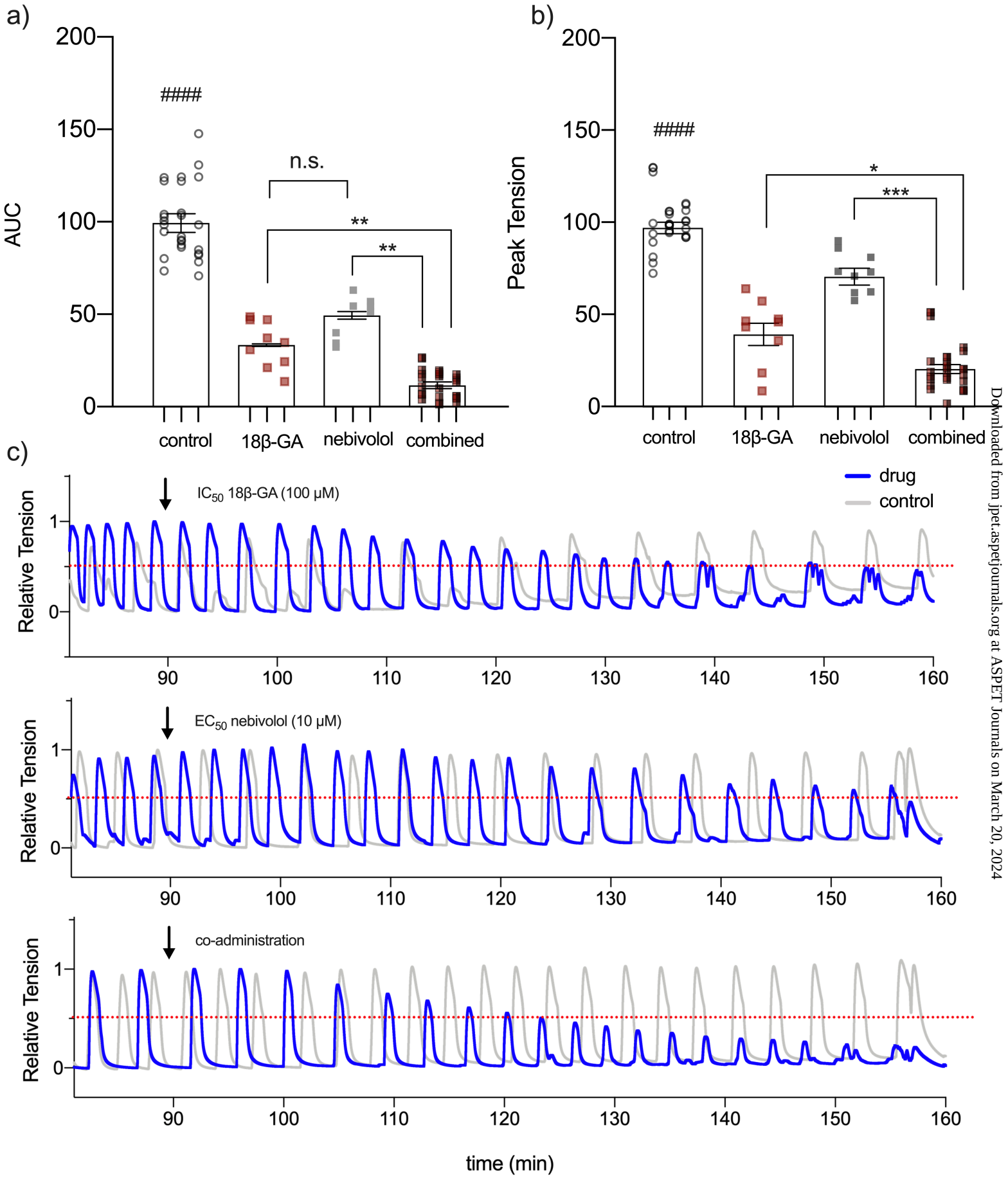

Figure 6

JPET-AR-2020-000427R1

Supplemental Materials

Novel Tocolytic Strategy: Modulating Cx43 Activity by S-Nitrosation

Scott D. Barnett, Hazik Asif, Mitchell Anderson, and Iain L. O. Buxton

Department of Pharmacology, Center for Molecular Medicine, University of Nevada, Reno School of Medicine, Reno, NV 89557

Figure S1. **Image panels of Cx43 expression in guinea pig and human myometrial tissue**. (a) 40µg of total protein lysate from guinea pig myometrium were isolated in MAPK buffer with protease and phosphatase inhibitors and a western blot was run on a 4-15% polyacrylamide gel and transferred to a nitrocellulose membrane and blocked in Licor® blocking buffer. Membranes were incubated with 1° Cx43 antibody followed by 2° Alexa Fluor 680, then normalized to GAPDH with 2° IRDye 800 antibody. (b) human myometrial samples were isolated and run in the same manner, except that Cx43 proteins were treated with a 2° IRDye 800 antibody, while GAPDH was treated with a 2° Alexa Fluor 680 antibody.

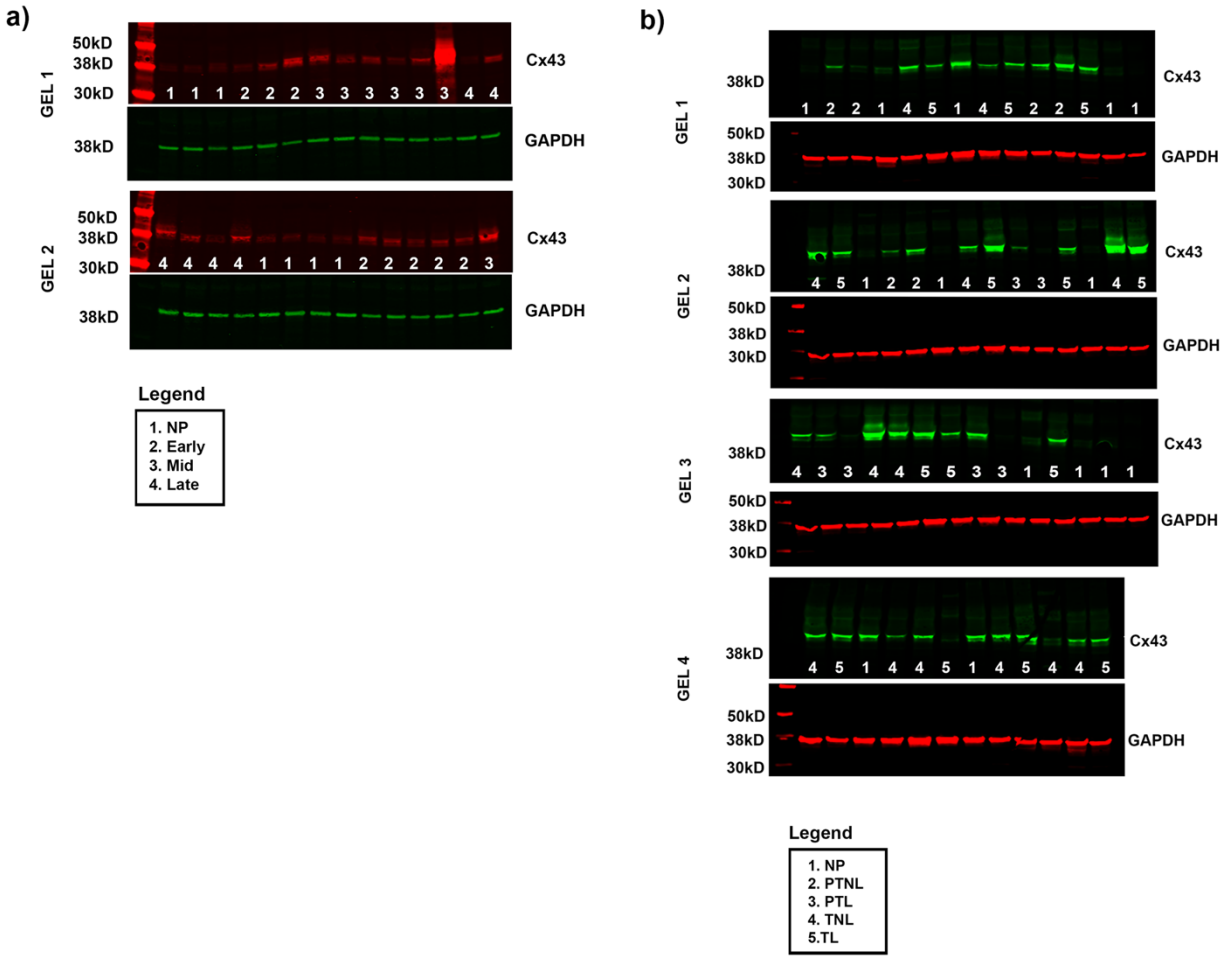

Figure S2. **Image panels of pS368-Cx43, Cx43-SNO, and total protein SNOs.** (a) After treatment with oxytocin (OT), or OT followed by nitric oxide (NO), human myometrial tissue was snap frozen in LN_2 and total protein was isolated in MAPK buffer with protease and phosphatase inhibitors and a western blot was run. Membranes were incubated with 1° Cx43-pS368 antibody followed by 2° Alexa Fluor 680, and the ratio of Cx43-pS368 was calculated against total Cx43 with 2° IRDye 800. (b) A biotin switch was conducted on human myometrial proteins with OT/NO treatment described in panel 'a', and the isolated S-nitrosated proteins were run on a western blot with 1° Cx43 antibody followed by 2° IRDye 800, but only after (c) total S-nitrosated proteins were detected using the reversible 2° Alexa Fluor total proteins stain, Licor Revert™.